Preprints of the 21st IFAC World Congress (Virtual)
Berlin, Germany, July 12-17, 2020

Extremum Seeking Control of a Three-Stage Anaerobic Digestion Model ⋆

Mihaela Sbarciog * **Alain Vande Wouwer** **
Jan Van Impe * **Laurent Dewasme** **

* *BioTeC+, Chemical and Biochemical Process Technology and Control Department of Chemical Engineering, KU Leuven, Belgium (e-mail: MihaelaIuliana.Sbarciog@kuleuven.be, Jan.VanImpe@kuleuven.be).*
** *Automatic Control Laboratory, University of Mons, Belgium (e-mail: Laurent.Dewasme@umons.ac.be, Alain.VandeWouwer@umons.ac.be)*

Abstract: Anaerobic digestion systems are of increasing interest as they are able to produce biogas while treating waste/wastewater. However, their dynamics is complex and not fully understood, which makes their operation and optimization difficult. In this paper, an extremum seeking control algorithm is applied to a three-stage anaerobic digestion system to maximize the outflow rate of methane. In a first stage, the stability analysis of the three-stage model is performed, which provides valuable information on the type of steady states the system possesses, the occurrence of the optimal steady state and good practices to successfully operate the system. In a second stage, an extremum seeking controller, which employs a recursive least-squares algorithm for block-oriented models, is implemented and tested on the anaerobic digestion model. Simulation results show that the proposed controller globally stabilizes the process dynamics at the optimal operating point. Compared to the classical extremum seeking algorithms, the proposed technique allows for a faster convergence, in an imposed time period assigned by the designer.

Keywords: Recursive Least Squares, Real-Time Optimization, Wiener-Hammerstein models, Process Control, Biogas Production.

1. INTRODUCTION

Anaerobic digestion (AD) is a well-established technology for producing renewable energy. The process involves several biochemical stages, through which organic matter found in waste or wastewater streams is transformed into biogas. This mainly consists of methane, carbon dioxide and hydrogen. The dynamics of an anaerobic digestion process is very complex and not fully understood, which makes its optimization and control difficult. In addition, some of the process key variables cannot be measured due to the lack of robust on-line measurement systems. In practice, most of the biogas producing plants are still operated manually (Gaida et al., 2017), resulting in a suboptimal biogas production.

To cope with the system complexity and develop efficient control structures, the research community relies on the use of models, which describe with various degrees of detail the process dynamics. Model analysis provides valuable information, which can be further used in the control design stage, resulting in simpler to implement control loops (Jimenez et al., 2015). Many studies have been published, most of them focusing on two-stage AD models (Sbarciog et al., 2010; Benyahia et al., 2012; Rincón et al., 2014; Khedim et al., 2018).

One of the main characteristics of the AD processes emphasized by the analysis studies is the steady state multiplicity. Hence, the start-up and control of AD processes is a delicate task due to the risk of reactor wash-out. This leads in current practice to the use of low dilution rates, and in turn to very slow transients and low biogas yield. To improve this situation, feedback control is an essential component, which is, however, difficult to implement as dynamic models are uncertain. It is therefore appealing to resort to model-free approaches, such as extremum seeking. Extremum seeking (ES) is a real-time feedback optimization technique initially proposed in the seminal work of Leblanc (1922), and brought back more recently to attention thanks to the filtering scheme of Ariyur and Krstic (2003). Its main purpose is to infer on-line information on the gradient of a convex and measurable cost function, and to drive this quantity to zero in average so as to reach the extremum. The main drawback of the ES approach is its inherent slow convergence due to the three-scale separation of the filtering technique (Ariyur and Krstic, 2003). Research efforts have therefore been paid to speed-up convergence. In (Guay and Dochain, 2015), a time-varying approach using a faster parameter estimator is proposed, while in (Guay and Dochain, 2017) an original proportional-integral controller replaces the classical integrator. However, parameter tuning mostly relies on empirical rules and can be tricky for the non-specialist user. In an attempt to alleviate this latter difficulty, Dewasme et al. (2011); Feudjio Letchindjio et al. (2018) used a Recursive Least Squares (RLS) algorithm to estimate the unknown static map parameters. Recently, Feudjio Letchindjio et al. (2019) proposed an original RLS strategy for block-oriented models (BOM, which can approach a wide range of nonlinear systems) taking system dynamics into account to drastically accelerate the ES estimator convergence. In the present study, the BOM-ES-RLS strategy is applied to optimize the biogas production of an anaerobic process described by a three-stage model, featuring multiple steady states and complex dynamics. Different extremum seek-

⋆ This work was supported by the ERA-NET FACCE-SurPlus FLEXIBI Project, co-funded by VLAIO project HBC.2017.0176.

ing techniques have been previously applied to two-stage AD models (Lara-Cisneros et al., 2015; Barbu et al., 2017). To our knowledge, this is the first reported implementation for a three-stage model, which brings up additional challenges.

2. MODEL DESCRIPTION

The model studied throughout this paper includes three stages of the anaerobic digestion process (Weedermann et al., 2013, 2015), acidogenesis, acetogenesis and methanogenesis, and involves four nutrient groups and the corresponding bacterial groups: simple substrates S, volatile fatty acids (except of acetic acid) V, acetic acid A, hydrogen H, acidogenic bacteria X_S, acetogenic bacteria X_V, acetoclastic methanogens X_A and hydrogenotrophic methanogens X_H. It is assumed that the biomass decay is negligible and it is not included in the model equations.

The three stage model is an approximation of the ADM1 model (Weedermann et al., 2015), as it is built by lumping the numerous components of ADM1 in only four microorganism groups growing on four substrates. The main advantage of this model is that it represents the complex dynamics of ADM1 with a reduced number of equations, allowing for a rigorous study of the system dynamics and the establishment of analytical results.

The model is based on the reaction network

$$k_1 S \xrightarrow{g_S} k_2 V + k_4 A + k_7 H + X_S \tag{1}$$

$$k_3 V \xrightarrow{g_V} k_5 A + k_8 H + X_V \tag{2}$$

$$k_6 A \xrightarrow{g_A} k_{10} CH_4 + X_A \tag{3}$$

$$k_9 H \xrightarrow{g_H} k_{11} CH_4 + X_H \tag{4}$$

In the first reaction, the acidogenic bacteria X_S grow on the organic substrate S and produce volatile fatty acids V, acetic acid A and hydrogen H. In the second reaction, the acetogenic bacteria X_V grow on volatile fatty acids V and produce acetic acid A and hydrogen H. In the third reaction, the acetoclastic methanogens X_A grow on the acetic acid and produce methane CH_4, while in the fourth reaction the hydrogenotrophic methanogens X_H grow on hydrogen and produce also methane.

The mass balances for each component in the bioreactor read:

$$\frac{dX_S}{dt} = -DX_S + g_S(S)X_S \tag{5}$$

$$\frac{dX_V}{dt} = -DX_V + g_V(V,H)X_V \tag{6}$$

$$\frac{dX_A}{dt} = -DX_A + g_A(A)X_A \tag{7}$$

$$\frac{dX_H}{dt} = -DX_H + g_H(H,A)X_H \tag{8}$$

$$\frac{dS}{dt} = D(S_{in} - S) - k_1 g_S(S)X_S \tag{9}$$

$$\frac{dV}{dt} = -DV + k_2 g_S(S)X_S - k_3 g_V(V,H)X_V \tag{10}$$

$$\frac{dA}{dt} = -DA + k_4 g_S(S)X_S + k_5 g_V(V,H)X_V - k_6 g_A(A)X_A \tag{11}$$

$$\frac{dH}{dt} = -DH + k_7 g_S(S)X_S + k_8 g_V(V,H)X_V - k_9 g_H(H,A)X_H \tag{12}$$

while the rate of methane production is given by:

$$Q_M = k_{10} g_A(A)X_A + k_{11} g_H(H,A)X_H \tag{13}$$

In (5)- (13), D represents the dilution rate (the inlet flow scaled by the reactor volume), S_{in} is the concentration of nutrient in the influent flow, k_i, $i = 1 \dots 9$ are the stoichiometric parameters, while g_j, $j \in \{S, V, A, H\}$ denote the growth functions. The growth functions depend on the concentration of the component that is decomposed and other factors that might inhibit the reaction:

$$g_S(S) = \frac{m_S S}{K_S + S} \tag{14}$$

$$g_V(V,H) = \frac{m_V V}{K_V + V + \mu_H H} \tag{15}$$

$$g_A(A) = \frac{m_A A}{K_A + A + A^2/K_I} \tag{16}$$

$$g_H(H,A) = \frac{m_H H}{K_H + H + \mu_A A} \tag{17}$$

where m_j and K_j, with $j \in \{S, V, A, H\}$ respectively denote the maximum growth rates and the half-saturation constants in the absence of inhibition; K_I is a coefficient describing the inhibition due to A on the growth of X_A; μ_H and μ_A are inhibition factors for the growth of X_V and X_H respectively due to H and A. The numerical values of the system parameters used in the simulation results are given in Table 1.

Table 1. Numerical values for system parameters

Parameter	Value	Parameter	Value
m_S	3.5 day^{-1}	k_1	11.111
K_S	0.4 g COD/L	k_2	1.962
m_V	0.86 day^{-1}	k_3	20
K_V	0.3 g COD/L	k_4	6.419
m_A	0.4 day^{-1}	k_5	10.357
K_A	0.15 g COD/L	k_6	20
K_i	10 g COD/L	k_7	2.367
μ_H	1 g COD/L	k_8	5.268
m_H	2.1 day^{-1}	k_9	16.667
K_H	2.5e-5 g COD/L	k_{10}	19
μ_A	5 g COD/L	k_{11}	15.667

2.1 Characterization of steady states

Analytical expressions for all system equilibria are provided by Sbarciog and Vande Wouwer (2016, 2020), however, their stability has been assessed only through simulations of system phase portraits for selected values of the dilution rate D and inlet substrate concentration S_{in}. Here, we provide a more formal analysis, which gives a global view on the steady states stability, in all possible regions (defined by the pair (S_{in}, D)) of the bifurcation diagram. The bifurcation diagram has been constructed analytically in (Sbarciog and Vande Wouwer, 2020) and is shown in Figure 1.

The model (5)-(12) exhibits a complex steady state behavior, comparable to the one of the ADM1 model (Bornhöft et al., 2013). Nine types of steady states may occur, characterized by:

(1) *Total wash-out*: there exists one steady state of this type, denoted by ξ^W, which is always physical, independent of the dilution rate and inlet substrate concentration;
(2) *Wash-out of the acetogenic bacteria and of both methanogenic microorganisms*: there exists one steady state of this type, denoted by ξ^0. This steady state is physical in all regions shown in Figure 1. Since no methanogens are present in the reactor, no methane is produced in this steady state.

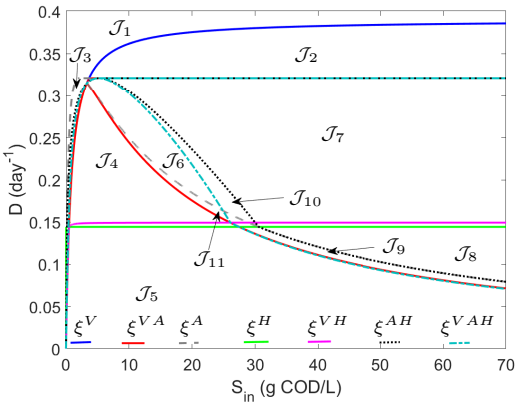

Fig. 1. Bifurcation diagram of the anaerobic digestion model

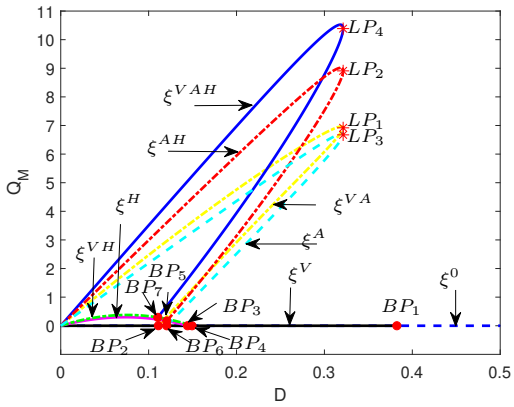

Fig. 2. Methane outflow rate at steady state

(3) *Wash-out of both methanogenic microorganisms*: one steady state of this type exists, denoted by ξ^V. This steady state is physical in the regions $\mathcal{J}_2$,$\mathcal{J}_4 - \mathcal{J}_{11}$. No methane is produced in this steady state.
(4) *Wash-out of hydrogenotrophic methanogens*: up to two steady states of this type may exist, denoted by ξ_i^{VA}, $i = 1, 2$. ξ_1^{VA} occurs in the regions $\mathcal{J}_4 - \mathcal{J}_{11}$, while ξ_2^{VA} occurs in the regions $\mathcal{J}_6 - \mathcal{J}_{11}$. These steady states are characterized by methane production through acetoclastic methanogenesis.
(5) *Wash-out of the acetogenic bacteria and acetoclastic methanogens*: one steady state of this type may exist, denoted by ξ^H. This steady state occurs as a physical equilibrium point in the regions $\mathcal{J}_5$, $\mathcal{J}_8$ and $\mathcal{J}_9$. Methane production is low in this steady state.
(6) *Wash-out of acetoclastic methanogens*: one steady state of this type may exist, denoted by ξ^{VH}. Methane production occurs through hydrogenotrophic methanogenesis, however the amount is low. This steady state is physical in the regions $\mathcal{J}_5$, $\mathcal{J}_8$ and $\mathcal{J}_9$.
(7) *Wash-out of the acetogenic bacteria*: up to two steady states of this type may occur, denoted by ξ_i^{AH}, $i = 1, 2$. ξ_1^{AH} is physical in the regions $\mathcal{J}_4 - \mathcal{J}_{11}$, while ξ_2^{AH} is physical only in $\mathcal{J}_7$, $\mathcal{J}_8$. Methane is produced through both acetoclastic and hydrogenotrophic methanogenesis.
(8) *Wash-out of acetogenic bacteria and hydrogenotrophic methanogens*: up to two steady states of this type may occur, denoted by ξ_i^{A}, $i = 1, 2$. ξ_1^{A} occurs in the regions $\mathcal{J}_3 - \mathcal{J}_{11}$, while ξ_2^{A} occurs in the regions $\mathcal{J}_6 - \mathcal{J}_8$ and $\mathcal{J}_{10}$. Methane is produced in these steady states.
(9) *Coexistence of all microorganisms types*: up to two steady states of this type may occur, denoted by ξ_i^{VAH}, $i = 1, 2$. The highest amount of methane is produced in these steady states, thus from a practical point of view the anaerobic digestion system should be operated around a steady state of this type. ξ_1^{VAH} is physical in the regions $\mathcal{J}_4 - \mathcal{J}_{11}$, while ξ_2^{VAH} is physical in $\mathcal{J}_7 - \mathcal{J}_{10}$.

Figure 2 shows the methane produced in each steady state type, for fixed inlet substrate concentration $S_{in} = 40$ COD/L and various values of the dilution rate. Maximum methane production occurs in a steady state type ξ^{VAH}, where all microorganisms types coexist in the bioreactor.

2.2 Stability of the steady states

The local stability of the steady states is assessed by linearizing the dynamics around the equilibrium points. To this end, one needs to compute the eigenvalues of the Jacobian matrix and evaluate them at the specific steady state. The determination of the Jacobian matrix and the calculation of the eigenvalues may be simplified by considering a transformation of the original system (5)-(12) to the so-called canonical states: $\xi = [\,\xi_a \;\; \xi_b\,]' \mapsto x = [\,x_a \;\; x_b\,]'$, with $x_a = \xi_a = [\,X_S \;\; X_V \;\; X_A \;\; X_H\,]'$ and x_b given by

$$x_b = \begin{bmatrix} S + k_1 X_S \\ V - k_2 X_S + k_3 X_V \\ A - k_4 X_S - k_5 X_V + k_6 X_A \\ H - k_7 X_S - k_8 X_V + k_9 X_H \end{bmatrix} \tag{18}$$

Then, state equations are rewritten as:

$$\dot{x}_1 = \frac{dX_S}{dt} = -Dx_1 + g_S(S)x_1 \tag{19}$$
$$\dot{x}_2 = \frac{dX_V}{dt} = -Dx_2 + g_V(V,H)x_2 \tag{20}$$
$$\dot{x}_3 = \frac{dX_A}{dt} = -Dx_3 + g_A(A)x_3 \tag{21}$$
$$\dot{x}_4 = \frac{dX_H}{dt} = -Dx_4 + g_H(H,A)x_4 \tag{22}$$
$$\dot{x}_5 = D(S_{in} - x_5) \tag{23}$$
$$\dot{x}_6 = -Dx_6 \tag{24}$$
$$\dot{x}_7 = -Dx_7 \tag{25}$$
$$\dot{x}_8 = -Dx_8 \tag{26}$$

and the Jacobian matrix can be written as

$$J = \begin{bmatrix} J_1 & J_2 \\ J_3 & J_4 \end{bmatrix} = \left[\begin{array}{c|ccc} J_1 & \multicolumn{3}{c}{J_2} \\ \hline -D & & & \\ 0 & -D & & \\ & & -D & \\ & & & -D \end{array}\right] \tag{27}$$

Note that the linear dynamics (23)-(26) is stable (negative eigenvalues equal to $-D$). Thus, the stability of the steady states is assessed by computing and evaluating the eigenvalues of the matrix J_1, which has the form

$$J_1 = \begin{bmatrix} j_1 & 0 & 0 & 0 \\ j_2 & j_3 & 0 & j_4 \\ j_5 & j_6 & j_7 & 0 \\ j_8 & j_9 & j_{10} & j_{11} \end{bmatrix} \tag{28}$$

The eigenvalues are the solutions of the equation

$$(j_1-\lambda)\left[\lambda^3-\lambda^2\left(j_3+j_7+j_{11}\right)+\lambda\left(j_3j_7+j_3j_{11}+\right.\right.$$
$$\left.\left.j_7j_{11}-j_9j_4\right)+j_3j_7j_{11}+j_6j_{10}j_4-j_9j_4j_7\right]=0 \quad (29)$$

with

$$j_1=-D+g_S-k_1x_1\frac{dg_S}{dS},\quad j_4=-k_9x_2\frac{\partial g_V}{\partial H} \quad (30)$$

$$j_3=-D+g_V+x_2\left(-k_3\frac{\partial g_V}{\partial V}+k_8\frac{\partial g_V}{\partial H}\right) \quad (31)$$

$$j_6=k_5x_3\frac{\partial g_A}{\partial A},\quad j_7=-D+g_A-k_6x_3\frac{\partial g_A}{\partial A} \quad (32)$$

$$j_9=x_4\left(k_8\frac{\partial g_H}{\partial H}+k_5\frac{\partial g_H}{\partial A}\right),\quad j_{10}=-k_6x_4\frac{\partial g_H}{\partial A} \quad (33)$$

$$j_{11}=-D+g_H-k_9x_4\frac{\partial g_H}{\partial H} \quad (34)$$

Note that except for the total wash-out steady state ξ^W, the first eigenvalue $\lambda = j_1$ is negative. All the other equilibria occur when the dilution rate equals the growth function of the acidogenic microorganisms, i.e., $D = g_S$. This growth function is of Monod type, which implies that its derivative is always positive. Moreover, k_1 and x_1 denote respectively a stoichiometric parameter and the concentration of microorganisms, which are always positive.

Table 2 displays the stability of equilibria in the widest regions shown on the bifurcation diagram (Figure 1). When a steady state is unstable, its index (number of positive eigenvalues) is also indicated. Noticeably, the steady state ξ_1^{VAH}, characterized by the highest methane production as seen in Figure 2 is always stable. However, ξ_1^{VAH} is the only stable steady state of the system at either low influent substrate concentrations or low dilution rate values, which are rarely employed in practice. At higher inlet substrate concentrations and dilution rates, which allow processing a reasonable amount of waste and produce a significant amount of methane, the anaerobic digestion system is characterized by bistability: two system steady states are locally asymptotically stable. ξ_1^{VAH} preserves its stability properties, while either ξ^V (in regions $\mathcal{J}_6$, $\mathcal{J}_7$, $\mathcal{J}_{10}$, $\mathcal{J}_{11}$) or ξ^{VH} (in regions $\mathcal{J}_8$, $\mathcal{J}_9$) becomes stable. Note that from a practical point of view neither ξ^V nor ξ^{VH} are desirable. Hence, the role of the extremum seeking algorithm detailed in the next section is to stabilize the operation of the anaerobic digestion system at the unknown optimal steady state.

3. EXTREMUM SEEKING CONTROL

3.1 RLS extremum seeking with block-oriented model

A recursive least-squares algorithm (RLS) with forgetting factor proposed by Dewasme et al. (2011) with a block-oriented model representation as in (Feudjio Letchindjio et al., 2019) (see Figure 3) is proposed to optimize the biogas production by extremum seeking (ES). The anaerobic digester is considered as a Hammerstein model with a static map (similar to one of the steady state diagrams of Figure 2) followed by a first order (strictly proper and stable) transfer function describing system/sensor dynamics. Since measurements are collected at discrete times, a discrete form of the model is used and $G(s) = \frac{1}{1+\tau s}$ is considered in an equivalent discrete form using the matched pole-zero method, leading to $G(z) = \frac{K_1}{z-\alpha}$ with $K_1 = 1-\alpha$ and $\alpha = e^{-\frac{T_s}{\tau}}$, T_s being the sampling period.

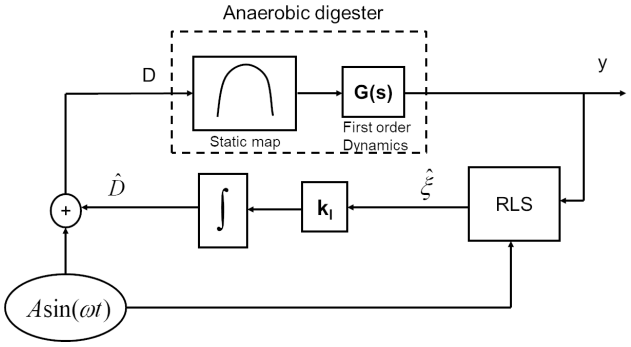

Fig. 3. Extremum seeking control loop applied to the anaerobic digester

The static map shown in Figure 2 is approximated by the linear form:

$$x(t_k) = c + \xi\, u(t_k) \quad (35)$$

where x is an intermediate state variable, $u = D$ the input, ξ the gradient and c a constant. The first order dynamics reads:

$$y(t_k) = K_1x(t_k) + \alpha y(t_{k-1}) \quad (36)$$

Combining (35) and (36) results in:

$$\begin{aligned} y(t_k) &= K_1\xi u(t_k) + \alpha y(t_{k-1}) + K_1c \\ &= \phi^T\theta + \nu \end{aligned} \quad (37)$$

where $\phi^T = [1, y(t_{k-1}), u(t_k)]^T$ is the known vector of explanatory variables, $\theta = [\theta_1, \theta_2, \theta_3]^T = [K_1c, \alpha, K_1\xi]^T$ is the parameter vector and $\nu \sim \mathcal{N}(0, \sigma^2)$ is white noise.

The RLS algorithm (see Figure 3) provides the gradient estimate $\hat{\xi} = \frac{\theta_3}{1-\theta_2}$ of ξ. The gradient estimation $\hat{\xi} \approx \widehat{\frac{\partial y}{\partial u}}$ is driven to zero in average by the extremum seeking control loop.

A dither signal $d = Asin(\omega t)$ is used to ensure the persistency of excitation (Åström and Wittenmark, 1995). As a general rule, a minimum of $\frac{n}{2}$ distinct sinusoids is necessary for the identification of n parameters (Landau and Dugard, 1986).

4. EXTREMUM SEEKING LOOP DESIGN

A simple pole-placement procedure can be used to define the extremum seeking control (ESC) closed-loop dynamics, i.e., to design the integral constant k_I (see Figure 3). As discussed by Feudjio Letchindjio et al. (2019), a controllable state-space representation of the slope/gradient evolution can be inferred as:

$$\xi_{k+1} = A\xi_k + Bw(D_{ref}) \quad (38a)$$
$$y = C\xi_k \quad (38b)$$

where w is a function of the corresponding input reference D_{ref} providing the desired gradient ξ_{ref}. Introducing an integral action, the system reads:

$$\begin{bmatrix}\xi_{k+1}\\ v_{k+1}\end{bmatrix} = \begin{bmatrix}A & 0\\ -CA & I\end{bmatrix}\begin{bmatrix}\xi_k\\ v_k\end{bmatrix} + \begin{bmatrix}B\\ -CB\end{bmatrix}w(D_{ref}) + \begin{bmatrix}0\\ I\end{bmatrix}r_{k+1} \quad (39a)$$

$$y = [C\ 0]\begin{bmatrix}\xi_k\\ v_k\end{bmatrix} \quad (39b)$$

Table 2. Steady states stability in the main regions of the bifurcation diagram: 's' - stable, 'u' - unstable, '-' - not physical

	$\mathcal{J}_1$	$\mathcal{J}_2$	$\mathcal{J}_3$	$\mathcal{J}_4$	$\mathcal{J}_5$	$\mathcal{J}_6$	$\mathcal{J}_7$	$\mathcal{J}_8$	$\mathcal{J}_9$	$\mathcal{J}_{10}$	$\mathcal{J}_{11}$
ξ^0	s	u(1)	u(1)	u(2)	u(3)	u(1)	u(1)	u(2)	u(3)	u(1)	u(2)
ξ^V	-	s	-	u(1)	u(2)	s	s	u(1)	u(1)	s	s
ξ_1^{VA}	-	-	-	u(1)	u(1)	u(1)	u(1)	u(1)	u(1)	u(1)	u(1)
ξ_2^{VA}	-	-	-	-	-	u(1)	u(2)	u(2)	u(2)	u(2)	u(1)
ξ^H	-	-	-	-	u(2)	-	-	u(1)	u(2)	-	-
ξ^{VH}	-	-	-	-	u(1)	-	-	s	s	-	-
ξ_1^{AH}	-	-	-	u(1)	u(1)	u(1)	u(1)	u(1)	u(1)	u(1)	u(1)
ξ_2^{AH}	-	-	-	-	-	-	u(2)	u(2)	-	-	-
ξ_1^{A}	-	-	s	u(2)	u(2)	u(2)	u(2)	u(2)	u(2)	u(2)	u(2)
ξ_2^{A}	-	-	-	-	-	u(2)	u(3)	u(3)	-	u(2)	-
ξ_1^{VAH}	-	-	-	s	s	s	s	s	s	s	s
ξ_2^{VAH}	-	-	-	-	-	-	u(1)	u(1)	u(1)	u(1)	-

Applying classical pole-placement procedures, the closed-loop dynamics can be specified in the time domain, yielding the integral (extremum seeking) control gain.

5. APPLICATION OF THE BOM-RLS-ES TO THE ANAEROBIC DIGESTER

The extremum seeking parameters are summarized in Table 3 (the reader is referred to Feudjio Letchindjio et al. (2019) concerning the RLS parametrization) and the results of the application of the BOM-RLS-ES controller to the anaerobic digester are shown in Figures 4, 5 and 6. During the first simulated days, the input is set to $D = 0.1$ d^{-1} to let the system reach a steady state. This steady state can be computed using the equilibria expressions provided by Sbarciog and Vande Wouwer (2016). However, the precise values of the states at equilibrium are not of interest. The most important fact is that for the chosen dilution rate and inlet substrate concentration ($S_{in} = 40$ gCOD/L), the anaerobic digestion system is operated in the region $\mathcal{J}_5$ (Figure 1), where the only stable steady state is of ξ^{VAH} type (see Table 2). This ensures that all microorganisms are present in the bioreactor at the moment the extremum seeking algorithm is started, rendering possible the maximization of methane outflow rate.

Figure 4 shows that the system natural settling time is approximately 50 d. In order to maintain the process dynamics and to avoid the slow convergence of the extremum seeking controllers (Guay and Dochain, 2015; Ariyur and Krstic, 2003; Feudjio Letchindjio et al., 2019), the same settling time (50 d) is imposed to the closed-loop system. This is achieved with an integral gain $k_I = 3.5 \times 10^{-5}$. Since 3 parameters from (37) are estimated, the dither signal is chosen as the sum of two sinusoids (allowing to identify up to 4 parameters) $d = A_1 sin(\omega_1 t) + A_2 sin(\omega_2 t)$ and the measurement sampling time is set to $T_s = 0.01$ d. To obtain more details on the dither signal parameter design, the reader may refer to Feudjio Letchindjio et al. (2019).

Table 3. Extremum seeking control parameters

k_I	$3.5\ 10^{-5}$	T_s	$0.01\ d$
A_1	$0.01\ d^{-1}$	ω_1	$\frac{2\pi}{5}\ d^{-1}$
A_2	$0.005\ d^{-1}$	ω_2	$\frac{2\pi}{2}\ d^{-1}$

In day 51, the ES controller is activated and leads the system to its optimal level of biogas production Q_M^*. As shown in Figure 5, and as expected from the pole-placement procedure, the convergence time is indeed approximately 50 d.

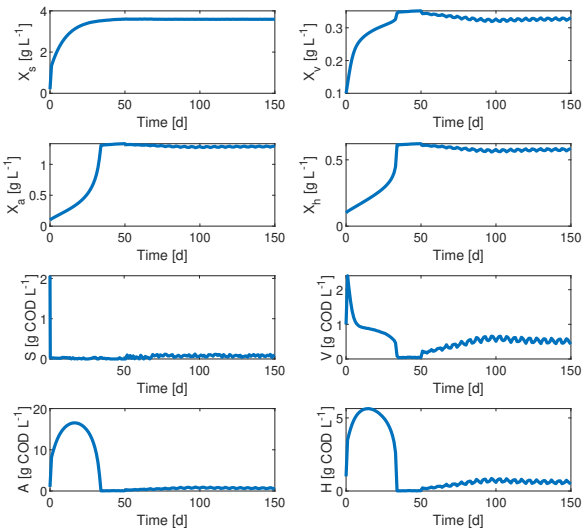

Fig. 4. Extremum seeking application to the anaerobic digester: time evolution of the system states

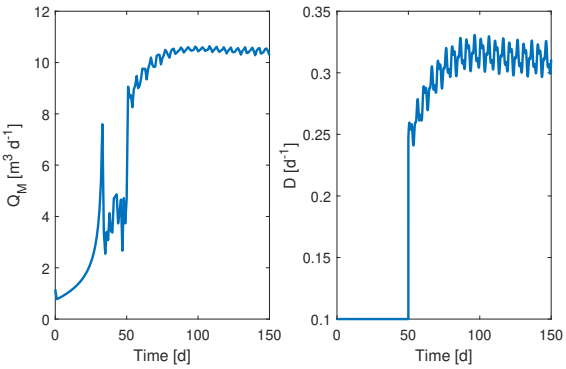

Fig. 5. Extremum seeking application to the anaerobic digester: time evolution of the output $y = Q_M$ and input $u = D$

6. CONCLUSION

In this paper the stability of a three-stage anaerobic digestion system is studied and the application of an extremum seeking control algorithm to maximize the outflow rate of methane is presented. The stability analysis shows that the optimal steady state for a fixed inlet substrate concentration lies in an operating

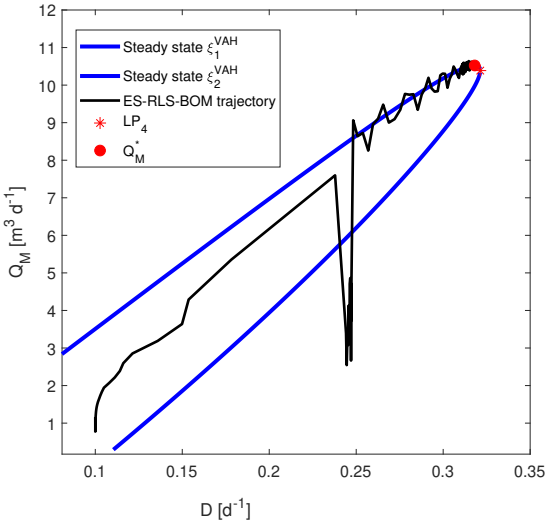

Fig. 6. Extremum seeking application to the anaerobic digester: convergence diagram

region where the system possesses two asymptotically stable steady states. The implemented extremum seeking (ES) control integrates a recursive least-squares (RLS) algorithm for block-oriented models (BOM), which allows for a faster convergence (compared to classical ES algorithms) to the optimal steady state. Simulation results show that the proposed controller stabilizes the system at the optimum, while the dynamics settles down in the imposed time. Future work will consider the evaluation of the closed-loop robustness with respect to parameter uncertainty and measurement noise.

REFERENCES

Ariyur, K.B. and Krstic, M. (2003). *Real-time Optimization by Extremum-seeking Control*. John Wiley & Sons, INC, wiley-interscience edition.

Åström, K. and Wittenmark, B. (1995). *Adaptive control*. Addison-Wesley Publishing Company.

Barbu, M., Ceanga, E., Vilanova, R., Caraman, S., and Ifrim, G. (2017). Extremum-seeking control approach based on the influent variability for anaerobic digestion optimization. *IFAC PapersOnLine*, 50-1, 12623–12628.

Benyahia, B., Sari, T., Cherki, B., and Harmand, J. (2012). Bifurcation and stability analysis of a two step model for monitoring anaerobic digestion processes. *Journal of Process Control*, 22, 1008–1019.

Bornhöft, A., Hanke-Rauschenbach, R., and Sundmacher, K. (2013). Steady-state analysis of the anaerobic digestion model no. 1 (ADM1). *Nonlinear Dynamics*, 73(1-2), 535–549.

Dewasme, L., Srinivasan, B., Perrier, M., and Vande Wouwer, A. (2011). Extremum-seeking algorithm design for fed-batch cultures of microorganisms with overflow metabolism. *Journal of Process Control*, 21(7), 1092–1104.

Feudjio Letchindjio, C.G., Deschenes, J.S., Dewasme, L., and Vande Wouwer, A. (2018). Extremum seeking based on a hammerstein-wiener representation. *IFAC-PapersOnLine*, 51(18), 744–749.

Feudjio Letchindjio, C., Dewasme, L., Deschenes, J.S., and Vande Wouwer, A. (2019). An extremum-seeking strategy based on block-oriented models: Application to biomass productivity maximization in microalgae cultures. *Industrial and Engineering Chemistry Research*, 58(30), 13481–13494.

Gaida, D., Wolf, C., and Bongards, M. (2017). Feed control of anaerobic digestion processes for renewable energy production: A review. *Renewable and Sustainable Energy Reviews*, 68, 869–875.

Guay, M. and Dochain, D. (2015). A time-varying extremum-seeking control approach. *Automatica*, 51, 356–363.

Guay, M. and Dochain, D. (2017). A proportional-integral extremum-seeking controller design technique. *Automatica*, 77, 61–67.

Jimenez, J., Latrille, E., Harmand, J., Robles, A., Ferrer, J., Gaida, D., Wolf, C., Mairet, F., Bernard, O., Alcaraz-Gonzalez, V., Mendez-Acosta, H., Zitomer, D., Totzke, D., Spanjers, H., Jacobi, F., Guwy, A., Dinsdale, R., Premier, G., Mazhegrane, S., Ruiz-Filippi, G., Seco, A., Ribeiro, T., Pauss, A., and Steyer, J.P. (2015). Instrumentation and control of anaerobic digestion processes: a review and some research challenges. *Reviews in Environmental Science and Bio/Technology*, 14, 615–648.

Khedim, Z., Benyahia, B., Cherki, B., Sari, T., and Harmand, J. (2018). Effect of control parameters on biogas production during the anaerobic digestion of protein-rich substrates. *Applied Mathematical Modelling*, 61, 351–376.

Landau, I.D. and Dugard, L. (1986). *Commande adaptative. Aspects practiques et theoriques*. Masson, Paris.

Lara-Cisneros, G., Aguilar-López, R., and Femat, R. (2015). On the dynamic optimization of methane production in anaerobic digestion via extremum-seeking control approach. *Computers and Chemical Engineering*, 75, 49–59.

Leblanc, M. (1922). Sur l'electrification des chemins de fer au moyen de courants alternatifs de frequence elevee. *Revue Générale de l'électricité*, 12(8), 275–277.

Rincón, A., Villa, J., Angulo, F., and Olivar, G. (2014). A dynamic analysis for an anaerobic digester: Stability and bifurcation branches. *Mathematical Problems in Engineering*, Article ID 514797.

Sbarciog, M., Loccufier, M., and Noldus, E. (2010). Determination of appropriate operating strategies for anaerobic digestion systems. *Biochemical Engineering Journal*, 51, 180–188.

Sbarciog, M. and Vande Wouwer, A. (2016). Bifurcation analysis of an anaerobic digestion system. In *Proceedings of ICSTCC*, 330–335. Sinaia, Romania.

Sbarciog, M. and Vande Wouwer, A. (2020). A constructive approach to assess the stability of anaerobic digestion systems. *Chemical Engineering Science*, submitted.

Weedermann, M., Seo, G., and Wolkowicz, G. (2013). Mathematical model of anaerobic digestion in a chemostat: effects of syntrophy and inhibition, journal of biological dynamics. *Journal of Biological Dynamics*, 7(1), 59–85.

Weedermann, M., Wolkowicz, G., and Sasara, J. (2015). Optimal biogas production in a model for anaerobic digestion. *Nonlinear Dynamics*, 81, 1097–1112.